

Refinability of splines derived from regular tessellations

Jörg Peters

September 24, 2018

Abstract

Splines can be constructed by convolving the indicator function of a cell whose shifts tessellate \mathbb{R}^n . This paper presents simple, non-algebraic criteria that imply that, for regular shift-invariant tessellations, only a small subset of such spline families yield nested spaces: primarily the well-known tensor-product and box splines. Among the many non-refinable constructions are hex-splines and their generalization to the Voronoi cells of non-Cartesian root lattices.

1 Introduction

Univariate uniform B-splines can be defined by repeated convolution, starting with the indicator functions¹ of the intervals or cells delineated by knots. This construction implies local support and delivers a number of desirable properties (see [dB78, dB87]) that have made B-splines the representation of choice in modeling and analysis. In particular, B-splines are refinable. That is, they can be exactly represented as a linear combinations of B-splines with a finer knot sequence. Refinability is a key ingredient of multi-resolution and adaptive and sparse representation of data. Refinability also guarantees monotone decay of error when shrinking the intervals.

By tensoring univariate B-splines, we can obtain splines on Cartesian grids in any dimension. Box-splines [dHR93] generalize tensoring by allowing convolution in directions other than orthogonal ones. As a prominent example in two variables, the linear 3-direction box-spline consists of linear pieces over each of six equilateral triangles surrounding one vertex. Shifts of this ‘hat function’ on an equilateral triangulation sum to one. Convolution of the hat function with itself results in a twice continuously differentiable function of degree 4; and m -fold convolution yields a function of degree $3m - 2$ with smoothness C^{2m} . Since this progression skips odd orders of smoothness, van der Ville et al. [vBU⁺04] proposed to directly convolve the indicator function of the hexagon and build splines customized to the

¹An indicator function takes on the value one on the interval but is zero otherwise.

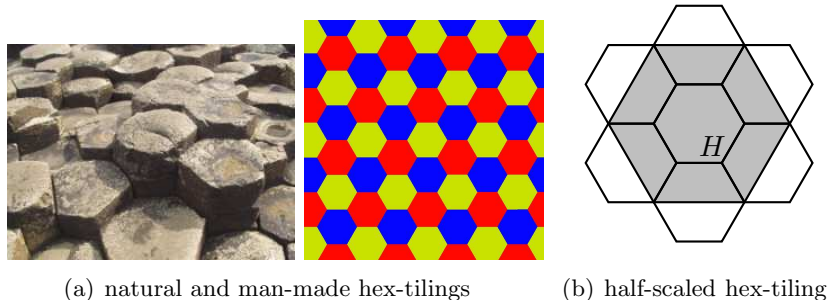


Figure 1: Hexagonal tessellations. (a) basalt formation and tiles (http://en.wikipedia.org/wiki/{Basalt,Hexagonal_tiling}) (b) Non-nesting of the hex partition in Example 1.

hexagonal tessellation of the plane (cf. Fig. 1a). They went on to show that the resulting hex-splines share a number of desirable properties familiar from box-splines. But the authors did not settle whether the splines were *refinable* [vdVU10], i.e. whether hex-splines of the given hexagonal tessellation T can be represented as linear combinations of hex-splines based on a scaled-down hexagonal tessellation, say $\frac{1}{2}T$. Generalizing the analysis of hex-splines,

- this paper presents simple non-algebraic criteria necessary for regular shift-invariant tessellations to admit refinable indicator functions.

For example, such a tessellation must contain, for every cell facet f , the plane through f . Therefore, requiring refinability, even of just the constant spline, strongly restricts allowable tessellations.

- In contrast to tensor-product and box splines, we show that hex-splines and similar constructions can only be *scaled*, *but not refined*: scaled hex-spline spaces are not nested.
- The analysis extends to overcomplete families (superpositions) of spline spaces.

The following example illustrates how non-refinability leads to loss of monotonicity of the approximation error under scaling: for one or more steps *halving the scale can increase the error*. By contrast, nested spaces guarantee monotonically decreasing error.

Example 1 Let \mathcal{H}^i be the space of indicator functions over a regular tessellation by hexagons of diameter 2^{-i} and such that, at each level of scaling, the origin is the center of one hexagon. Denote by H the indicator function in \mathcal{H}^0 whose support hexagon is centered at the origin. \mathcal{H}^1 does not contain a linear combination of functions that can replicate H since the supports of the six relevant scaled indicator functions are bisected by the boundary

of the support of H (see Fig. 1b). Correspondingly, the L^2 approximation error to H from \mathcal{H}^1 is $\frac{6}{2}A^1 > 0$ where A^1 is the area of the hexagon with diameter $\frac{1}{2}$. Since the error from \mathcal{H}^0 is by construction zero, the scaling by $1/2$ has increased the error. By carefully adding to H an increasing number of scaled-down copies, small increases in the L^2 error can be distributed over multiple consecutive steps. \square

Overview. Section 2 reviews tessellations induced by lattices, hex-splines and their generalizations. Section 3 exhibits two non-algebraic criteria, chosen for their simplicity, for testing whether a tessellation can support a refinable space of splines that are constructed by convolution of indicator functions of its cells. Section 4 extends this investigation to a multiple covering of \mathbb{R}^n by distinct families of indicator functions.

2 Splines from lattice Voronoi cells

A n -dimensional lattice is a discrete subgroup of full rank in a n -dimensional Euclidean vector space. Alternatively, such a lattice may be viewed as inducing a tessellation of space into identical cells without n -dimensional overlap². The tessellation is then generated by the translational shifts of one cell. For example, lattice points can serve as sites of Voronoi cells. The Euclidean plane admits three highly symmetric shift-invariant tessellations: partition into equilateral triangles, squares, or hexagons respectively. Repeated convolution starting with the indicator function of any of these polygons yields spline functions of local support and increasing degree. The regular partition into squares gives rise to uniform tensor-product B-splines and the regular triangulation and its hexagonal dual to box splines.

An interesting additional type of spline arises from convolving the indicator function H of the hexagon with itself. Such hex-splines, a family of C^{k-1} splines supported on a local $k + 1$ -neighborhood, were developed and analyzed by van De Ville et al. [vBU⁺04]. That paper compares hex-splines to tensor-product splines and uses the Fourier transform of hex-splines to derive, for low frequencies, the L^2 approximation order, as a combination of the projection into the hex-spline space and a quasi-interpolation error. [CvB05] derived quasi-interpolation formulas and showed promising results when applying hex-splines to the reconstruction of images (see also [CvU06, Cv07, Cv08]). Van De Ville et al. [vBU⁺04]. also observed that hexagons are Voronoi cells of a lattice and that the cell can be split into three quadrilaterals, using one of two choices of the central split. Thus H can be split into three constant box splines whose mixed convolution yields higher-order splines [Kim08b, ME10]. However, while box-splines are refinable, we will see that hex-splines are not refinable in a shift-invariant way.

² A common convention is to define the cells to be half-open sets so that they do not overlap on facets, but nevertheless cover.

3 Refinability constraints

We consider a polyhedral tessellation T of \mathbb{R}^n into unpartitioned n -dimensional units, called *cells*, that are bounded by a finite number of $n - 1$ -dimensional facets. We denote by $\chi(T)$ the space of indicator functions of the cells of T and by $\chi(T^1)$ the space of indicator functions on some scaled-down copy T^1 of T . The space $\chi(T)$ is *refinable* if each indicator function in $\chi(T)$ can be represented as a linear combination of functions in $\chi(T^1)$.

Establishing whether a tessellation T admits a refinable space of indicator functions therefore requires proving the existence of weights such that a linear combination of elements in $\chi(T^1)$ with these weights reproduces each element in $\chi(T)$. Proposition 1 below provides a much simpler *necessary condition* that avoids such algebraic analysis. While our focus is on shift-invariant tessellations, Proposition 1 applies more generally and also to cell boundaries of co-dimension greater than 1. Its proof uses the notion of a $c^1 \in T^1$ straddling a facet of a cell $c \in T$. A cell c^1 *straddles* a facet f of c if there exists a point \mathbf{p} on f , a unit vector \mathbf{n} normal to f at \mathbf{p} and $\epsilon > 0$ such that both $\mathbf{p} + \epsilon\mathbf{n} \in c^1$ and $\mathbf{p} - \epsilon\mathbf{n} \in c^1$.

Proposition 1 *Let T be a polyhedral tessellation of \mathbb{R}^n and T^1 its scaled-down copy. Then $\chi(T)$ is refinable only if every facet of T is the union of facets of T^1 .*

Proof Assume that a facet f of a cell c in T is not a union of facets of T^1 . Then, since T^1 is a tessellation, some cell c^1 of T^1 must straddle f . Let $H^1 \in \chi(T^1)$ be the indicator function of c^1 and H the indicator function of c . Then, in order to reproduce the unit step of H across f , H^1 must simultaneously take on both the value 0 and the value 1. |||

Translation-invariant or shift-invariant tessellations are a special case of transitive tilings where every cell can be mapped to every other cell by translation, without rotation.

Proposition 2 *If T is a shift-invariant tessellation, $\chi(T)$ is refinable only if, T contains, for each facet f , the hyperplane through f .*

Proof The coarser-scaled copies of T contain enlarged copies of every facet in T . By Proposition 1 these copies must be a union of facets of T . Therefore a *shifted copy* of every facet is strictly contained in the interior of and so extended by some coarser facet. Shift-invariance then implies that *every* facet f lies strictly inside such an extension. Ever coarser tessellations provide a sequence of extensions of f in any direction by any amount. |||

By inspection of the three regular tessellations of the plane, only the Cartesian grid and the uniform triangulation satisfy Proposition 2, but not the partition into hexagons.

Corollary 1 *Hex splines are not refinable.*

We can generalize this observation by simplifying the inspection criterion.

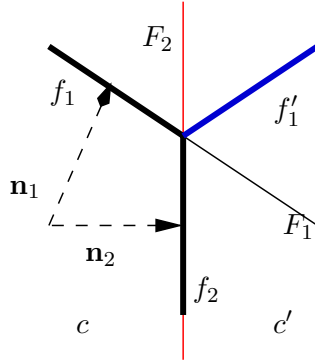


Figure 2: A pair of facets f_1, f_2 of a cell c meet with an obtuse angle: the outward pointing normals $\mathbf{n}_1, \mathbf{n}_2$ (dashed) have a strictly positive inner product.

We say that two abutting facets f_1 and f_2 of a cell c meet with an obtuse angle if, for $i = 1, 2$, there exist unit vectors \mathbf{n}_i orthogonal to f_i and outward pointing so that $\mathbf{n}_1 \cdot \mathbf{n}_2 > 0$.

Proposition 3 *Let T be a tessellation of \mathbb{R}^n by shifts of one polyhedral cell c . If two facets f_1 and f_2 of c meet with an obtuse angle and if c' , the reflection of c across f_2 , is a cell of T then $\chi(T)$ is not refinable.*

Proof Assume $\chi(T)$ is refinable under the given conditions. Let c' be the reflection of c across (the plane through) f_2 . Since c' must not overlap c , obtuse angles exceeding π , such as the reentrant corner of an L-shaped cell, cannot occur in c . Denote by f'_1 the reflection of f_1 across f_2 and by e the common intersection of f_1, f_2 and f'_1 (see Fig. 2).

Within c' , by reflection, the facets f_2 and f'_1 meet at e with an obtuse angle. By Proposition 2 the extension F_1 of f_1 lies in T . Since the outward-pointing normal of f_2 with respect to c' is $-\mathbf{n}_2$, f_2 and F_1 meet at e with an acute angle. Therefore F_1 extends f_1 into and splits c' . This contradicts the definition of a cell as an unpartitioned unit and hence the initial assumption.

|||

The next Proposition 3 allows us to quickly decide which of the (symmetric crystallographic) root lattices $\mathcal{A}_n, \mathcal{A}_n^*, \mathcal{B}_n, \mathcal{D}_n, \mathcal{D}_n^*, \mathcal{E}_j, j = 6, 7, 8$ [CS98] are suitable for building refinable splines by convolution of their nearest-neighbor (Voronoi) cells.

Corollary 2 *Splines obtained by convolving the Voronoi cell of a non-Cartesian crystallographic root lattice are not refinable.*

Proof We test whether the Voronoi cells of the root lattices contain a pair of abutting faces that meet with an obtuse angle. We may assume that one Voronoi site (cell center) is at the origin. By definition of a Voronoi cell, the position vectors \mathbf{n}_1 and \mathbf{n}_2 of two adjacent nearest neighbors, as identified by their root system, are normal to the corresponding abutting bisector facets. Therefore these facets meet with an obtuse angle if $\mathbf{n}_1 \cdot \mathbf{n}_2 > 0$.

The \mathcal{A}_n lattice is traditionally defined via an embedding in \mathbb{R}^{n+1} , $n > 1$. More convenient for our purpose is the alternative geometric construction in \mathbb{R}^n via the $n \times n$ generator matrix $\mathbf{A}_n := \mathbf{I}_n + \frac{c_n}{n} \mathbf{J}_n$ of Theorem 1 of [KP10]. Here \mathbf{I}_n is the identity matrix, \mathbf{J}_n the $n \times n$ matrix of ones and $c_n := \frac{-1 + \sqrt{n+1}}{n}$. Denoting the i th coordinate vector by \mathbf{e}_i , we choose \mathbf{e}_1 and $\mathbf{e}_1 + \mathbf{e}_2$ on the Cartesian grid, and map them via \mathbf{A}_n to the nearest \mathcal{A}_n neighbors of the origin. The inner product of the images of \mathbf{e}_1 and $\mathbf{e}_1 + \mathbf{e}_2$ is

$$\mathbf{A}_n \mathbf{e}_1 \cdot \mathbf{A}_n (\mathbf{e}_1 + \mathbf{e}_2) = \frac{n + 4c_n + c_n^2}{n} = \frac{2}{n} (n + \sqrt{n+1} - 1) > 0.$$

For the \mathcal{A}_n^* lattice, the computation is identical except that $c_n := \frac{-1 + \frac{1}{\sqrt{n+1}}}{n}$. The inner product is $\frac{1}{n(n+1)} (n^2 - 2n - 2 + 2\sqrt{n+1}) > 0$.

For the \mathcal{D}_n lattice, defined in $n \geq 3$ dimensions, the generator matrix is $\mathbf{D}_n := \begin{bmatrix} \mathbf{I}_{n-1} & -\mathbf{e}_{n-1}^{n-1} \\ -\mathbf{j}_{n-1}^t & -1 \end{bmatrix}$ (see e.g. Section 7 of [KP11]) and

$$\mathbf{D}_n \mathbf{e}_1 \cdot \mathbf{D}_n (\mathbf{e}_1 + \mathbf{e}_2) = 3 > 0.$$

Since \mathbf{D}_n^{-t} is the generator of \mathcal{D}_n^* , the inner product for \mathcal{D}_n^* is 2.

For \mathcal{B}_n , the Cartesian cube lattice has an inner product of 0 identifying its uniform tensor-product B-spline constructions as potentially refinable (which indeed they are). On the other hand, splitting each cube by adding the diagonal directions of the full root system [Kim08a] yields the inner product $\mathbf{e}_1 \cdot \mathbf{j} = 1$.

For \mathcal{E}_6 , we select the root vectors $(1, 1, 0, 0, 0, 0)$ and $(1, 1, 1, 1, 1, \sqrt{3})/2$ with inner product 1. For \mathcal{E}_7 , we select the root vectors $(1, 1, 0, 0, 0, 0, 0)$ and $(1, 1, 1, 1, 1, 1, \sqrt{2})/2$ with inner product 1. For \mathcal{E}_8 , we select the root vectors $(1, 1, 0, 0, 0, 0, 0, 0)$ and $\mathbf{j}_8/2$ with inner product 1. |||

The equilateral triangulation in \mathbb{R}^2 is dual to the ‘honeycomb lattice’ which is not a standard lattice. The equilateral triangulation yields an inner product of $\frac{-1}{2}$ compatible with refinability and indeed plays host to the refinable ‘hat’ function.

4 Overcomplete spaces

Since the evaluation of hex-splines by convolving three families of box splines already makes use of a large number of terms, it is reasonable to investigate

whether superposition of several families of hex-splines are refinable as a family. That is, we consider a family of distinct shift-invariant tessellations $\{T_j\}_{j=0..J}$ obtained by shifts of T_0 . Their union covers \mathbb{R}^n $J+1$ -fold. We check refinability of the family, i.e. whether each member of the family can be expressed as a linear combination of the scaled-down copies of splines of the family. Example 2 makes this concrete for $J=2$.

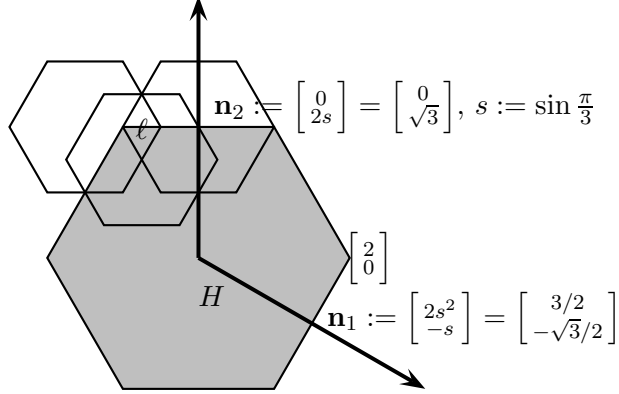


Figure 3: A lozenge-shaped pair of triangles ℓ is in the common support of three half-scaled translated copies of the grey hexagon h .

Example 2 Denote by T_0 a tessellation of the plane into unit-sized hexagons and by T_1 and T_2 its shifts by integer multiples of $\frac{1}{2}\mathbf{n}_1$ and $\frac{1}{2}\mathbf{n}_2$ (see Fig. 3). Let $H \in \chi(T_0)$ be the indicator function of the unit hexagon h centered at the origin. Consider the three $\frac{1}{2}$ -scaled, translated copies of h shown in Fig. 3. The three copies intersect in a lozenge-shaped pair of triangles ℓ . No other shifts of the $\frac{1}{2}$ -scaled hexagons in T_0 , T_1 or T_2 overlap ℓ . Therefore any linear combination of indicator functions in $\{T_j\}_{j=0..J}$ has a single value on ℓ . Since ℓ straddles the boundary of h , this constant linear combination would have to be simultaneously 1 and 0 to replicate H . \square

Example 2 suggests the following generalization of Proposition 2. A *superposition* T of a family of shift-invariant tessellations $\{T_j\}_{j=0..J}$ of \mathbb{R}^n is the tessellation obtained by partitioning \mathbb{R}^n by all cell facets in any of the tessellations T_j . T differs from $\{T_j\}_{j=0..J}$ in that it contains fractions or *pieces* of the original cells.

Proposition 4 *Given a family $\{T_j\}_{j=0..J}$ of polyhedral shift-invariant tessellations of \mathbb{R}^n , the space of indicator functions $\bigcup_{j=0..J} \chi(T_j)$ is refinable only if the superposition T of $\{T_j\}_{j=0..J}$ contains, for each facet f , the hyperplane through f .*

Proof Assume that $\bigcup_{j=0..J} \chi(T_j)$ is refinable. Assume additionally that a scaled-down copy T^1 of T contains an unpartitioned piece $c^1 \in T^1$ that

straddles a facet f of some cell c in one of the T_j . Analogous to the proof of Proposition 1, any linear combination of the indicator functions of the family $\{T_j\}_{j=0..J}$ that replicates the step of the indicator function on c across f would have to be simultaneously 0 and 1 on c^1 . Therefore every facet of T must be a union of facets of T^1 . Analogous to the proof of Proposition 2, the claim follows by considering ever coarser-scaled copies of the T_j and hence of T . $\parallel\parallel\parallel$

Example 3 illustrating Proposition 5 shows that Proposition 4 does not yield a sufficient constraint. In generalizing Proposition 3 to overcomplete spline families, we restrict attention to families of tessellations that minimize facet overlap.

Definition 1 (efficient family of tessellations) *A family of tessellations $\{T_j\}_{j=0..J}, T_j \in \mathbb{R}^n$ is efficient if the intersection of more than two cell facets is of co-dimension greater than 1.*

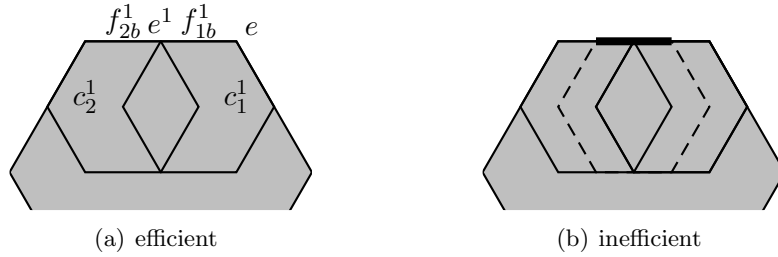


Figure 4: (a) Two scaled-down shifts of a hexagon cover the top facet (edge) of the original hexagon exactly once from inside (gray region) and hence twice if we continue the tessellation by reflection across the facet. Adding the dashed scaled-down hexagon in (b) covers a part of the top (thick edge) twice from inside so that reflection yields an inefficient family of tessellations.

Proposition 5 *Let $\{T_j\}_{j=0..J}$ be an efficient family of tessellations of \mathbb{R}^n by shifts of one polyhedral cell $c \in T_0$. If two facets f_a and f_b of c meet with an obtuse angle α and no facet of c meets f_b with an angle less than $\pi - \alpha$, and if c' , the reflection of c across f_b , is a cell of T_0 then $\bigcup_{j=0..J} \chi(T_j)$ is not refinable.*

Proof Assume $\bigcup_{j=0..J} \chi(T_j)$ is refinable. Let e be the $n - 2$ dimensional intersection of two facets f_a and f_b of the cell c . By Proposition 4, there exist $c_1^1, c_2^1 \in \{T_j^1\}_{j=0..J}$ whose two facets f_{1b}^1 and f_{2b}^1 lie on f_b , whose shared boundary e^1 is parallel to e (for $n = 2$, e^1 is a point) and that lie both to the same side of f_b as c . Without loss of generality, f_{1b}^1 is closer to e than is f_{2b}^1 (cf. Fig. 4a). When $n = 2$, we set $\mathbf{p} = e^1$ and when $n > 2$, we pick a point \mathbf{p} in the interior of e^1 .

Due to efficiency, of all cells in $\{T_j^1\}_{j=0..J}$ that have one facet on f_b and lie to the same side as c , exactly three pieces of the superposition T^1 of $\{T_j^1\}_{j=0..J}$ meet at \mathbf{p} : the piece i_1 solely inside c_1^1 , the piece i_2 solely inside c_2^1 , and i_\cap , the n -dimensional intersection of c_1^1 and c_2^1 . The intersection i_\cap exists and is n -dimensional due to the obtuse angle α of c at e and hence of c_2^1 at e^1 ; and because c and hence c_1^1 forms no angle less than $\pi - \alpha$ with f_b . By reflection across f_b , there are three analogous pieces o_j outside c at \mathbf{p} . Fig. 5a illustrates the situation in the 2-dimensional plane \mathcal{P} through \mathbf{p} and orthogonal to e^1 .

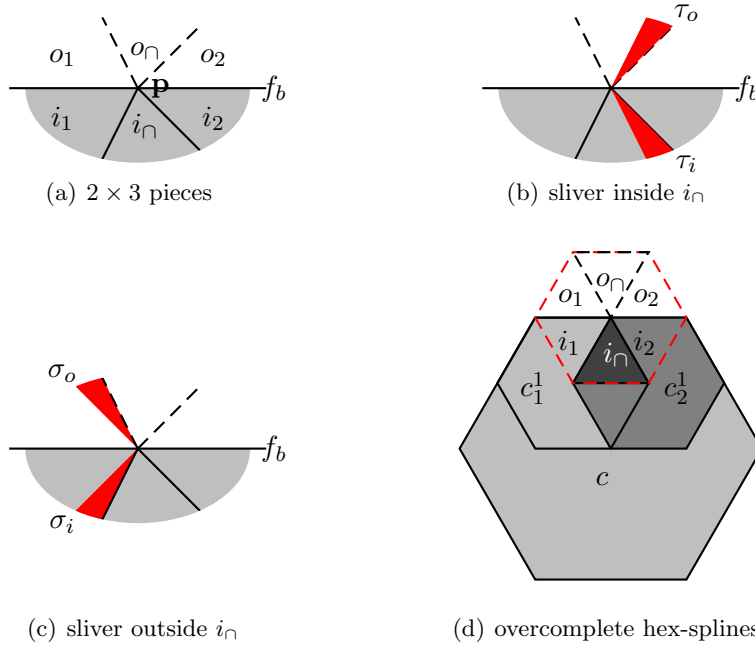


Figure 5: Pieces (a) and slivers (red in b,c) in the plane \mathcal{P} . (d) Concrete partition of Example 3 into pieces (sectors) of a neighborhood of point \mathbf{p} on the partition of a facet f_b of the support cell c of H .

Denote by s the spline formed as a linear combination of indicator functions of the cells in $\{T_j^1\}_{j=0..J}$ that have one facet on f_b . To replicate the indicator function of c , s must have a unit step across f_b and hence $s(i_1) - s(o_1) = 1$ and $s(i_2) - s(o_2) = 1$ where s applied to a piece of T^1 means evaluating s at some point in that piece, sufficiently close to \mathbf{p} . Due to the overlap of the indicator functions on i_\cap and on o_\cap , at \mathbf{p}

$$s(i_\cap) - s(o_\cap) = s(i_1) + s(i_2) - s(o_1) - s(o_2) = 2, \quad (1)$$

incompatible with the unit step across f_b at \mathbf{p} .

Additional cells of $\{T_j^1\}$ that overlap all six pieces, $i_1, o_1, i_\cap, o_\cap, i_2, o_2$, surrounding \mathbf{p} do not affect the above difference since their indicator

functions are constant. It remains to consider cells with facets crossing \mathbf{p} and it suffices to consider the 2-dimensional plane \mathcal{P} through \mathbf{p} and orthogonal to e^1 . In \mathcal{P} , as shown in Fig. 5a,b,c, let the boundary (i_\cap, i_2) between i_\cap and i_2 form a smaller-or-equal angle with f_b than the boundary (i_\cap, i_1) . Due to efficiency, within c , crossing facets lie either (b) strictly inside i_\cap or (c) strictly outside i_\cap since the boundaries must not be covered a third time. In case (b) this strictness implies the existence of a sliver τ_i , i.e. a piece of T^1 devoid of crossing facets, attached to (i_\cap, i_2) and inside i_\cap . Any linear combination of indicator functions corresponding to cells with crossing facets of type (b) therefore leaves unchanged the difference in value and hence the incompatibility (1), between τ_i and its reflection τ_o across f_b (see Fig. 5b). In case (c), any linear combination of indicator functions that modifies the value in i_\cap also modifies the difference in value between two slivers σ_i and σ_o , where σ_i is attached to (i_\cap, i_1) and lies inside i_1 and σ_o is its reflection across f_b . Specifically, when the value of $s(i_\cap) - s(o_\cap)$ is changed to satisfy the step condition, $s(\sigma_i) - s(\sigma_o)$ is changed away from the prescribed value 1. Together this contradicts the assumption that $\bigcup_{j=0..J} \chi(T_j)$ is refinable. \square

The following Example 3 illustrates Proposition 5.

Example 3 Consider, as in Fig. 5d, shifts

$$H_1(x) := H(x - \begin{bmatrix} -c \\ s \end{bmatrix}), \quad H_2(x) := H(x - \begin{bmatrix} c \\ s \end{bmatrix}), \quad c := \cos \frac{\pi}{3}, \quad s := \sin \frac{\pi}{3}$$

of the indicator function $H(x)$ of a tessellation T_0 . The three corresponding tessellations intersect only in single triangles and their superposition contains no piece that straddles the support hexagon of H . Yet this minimal family³ is, as expected, not refinable. Fig. 5b shows the regions i_\cap and o_\cap where, for any spline s , $s(i_\cap) - s(o_\cap) = 2$ since $s(i_1) - s(o_1) = 1$ and $s(i_2) - s(o_2) = 1$. \square

The proof of Corollary 2 showed that a pair of facets of the Voronoi cells of non-Cartesian crystallographic lattices form obtuse angles. By the symmetry of the cells, all facet angles are obtuse and hence satisfy the angle criteria of Proposition 5. Together with the reflection symmetry of the lattices, Proposition 5 implies the following generalization of Corollary 2.

Corollary 3 *Efficient overcomplete families of splines obtained by convolution of the Voronoi cell of a non-Cartesian crystallographic root lattice are not refinable.*

³ $J = 2$ yields the minimal number of scaled families that can satisfy the necessary constraints of Proposition 4 for hex-splines for three reasons. First, scaling should at least be binary. Second, the family that includes $H/2$ does not contribute to the step function because its cells straddle the boundary of c if they include a part of the boundary (see the dashed hexagon in Fig. 5d). Third, at least two $\frac{1}{2}$ -scaled edges, namely of elements of T_1^1 and T_2^1 , are required to cover any edge of H .

5 Conclusion

The paper identified several necessary criteria for tessellations to admit a refinable space of (convolutions of) indicator functions. The criteria are chosen for their simplicity. For example, we showed that admissible shift-invariant tessellations must contain, for every facet, the whole plane through that facet. Already for hex-splines and hex-spline superpositions, an alternative algebraic proof of non-refinability is considerably more involved.

Corollary 2 and 3 show that the increased isotropy of the Voronoi cells of non-Cartesian root lattices prevents refinability, even for overcomplete spaces obtained by efficient superposition of shifted lattices. Increased isotropy of the Voronoi cells is however the main reason for considering non-Cartesian lattices in the first place: these lattices have high packing densities that can improve sampling efficiency [PM62].

In conclusion, if we seek shift-invariant refinable classes of splines from convolving indicator functions of polyhedral cells, remarkably few options exist apart from tensor-product B-splines and box-splines. This does not imply that more general lattices fail to have associated refinable splines that represent their symmetry and translational structure. In the bivariate setting, odd orders of continuity on the hexagonal dual of the regular triangulation can be filled in by half-box splines [PB02]. And if fractal support is acceptable, [OS03, HR02] provide refinable functions with approximately hexagonal footprint. Combining families of symmetric box-splines, such as [KP11] yields refinable splines for any level of smoothness and crystallographic structure. It is just the particular approach of convolving non-Cartesian lattice Voronoi cells that fails to provide the important spline property of refinability.

Acknowledgement Zhangjin Huang kindly worked out a first, algebraic proof of non-refinability for Example 2, a scenario I posed to him. Andrew Vince and Carl de Boer helped me clarify the exposition in its early stages.

References

- [CS98] J. H. Conway and N. J. A. Sloane. *Sphere Packings, Lattices and Groups*. Springer-Verlag New York, Inc., New York, NY, USA, 3rd edition, 1998.
- [Cv07] L. Condat and D. van de Ville. Quasi-interpolating spline models for hexagonally-sampled data. *IEEE Trans. Image Processing*, 16(5):1195–1206, May 2007.
- [Cv08] L. Condat and D. van de Ville. New optimized spline functions for interpolation on the hexagonal lattice. In *ICIP*, pages 1256–1259, 2008.
- [CvB05] L. Condat, D. van de Ville, and T. Blu. Hexagonal versus orthogonal lattices: A new comparison using approximation theory. In *ICIP*, pages III: 1116–1119, 2005.

- [CvU06] L. Condat, D. van de Ville, and M. Unser. Efficient reconstruction of hexagonally sampled data using three-directional box-splines. In *ICIP*, pages 697–700, 2006.
- [dB78] C. de Boor. *A Practical Guide to Splines*. Springer, 1978.
- [dB87] C. de Boor. B-form basics. In G. Farin, editor, *Geometric Modeling: Algorithms and New Trends*, pages 131–148. SIAM, 1987.
- [dHR93] C. de Boor, K. Höllig, and S. Riemenschneider. *Box splines*. Springer-Verlag New York, Inc., New York, NY, USA, 1993.
- [HR02] B. Han and S. Riemenschneider. Interpolatory biorthogonal wavelets and cbc algorithm. In *Wavelet Analysis and Its Applications*, D. Deng, D. Huang, R.Q. Jia, W. Lin, J Wang, Eds, pages 119–139. AMS, 2002.
- [Kim08a] M. Kim. *Symmetric box-splines on root lattices*. PhD thesis, University of Florida, August 2008.
- [Kim08b] M. Kim. E-mail and pdf draft to A Entezari and J Peters, April 09 2008.
- [KP10] M. Kim and J. Peters. Symmetric box-splines on the \mathcal{A}_n^* lattice. *J. of Approximation Theory*, 162(9):1607–1630, September 2010.
- [KP11] M. Kim and J. Peters. Symmetric box-splines on root lattices. *Journal of Computational and Applied Mathematics*, 235(14):3972–3989, May 2011.
- [ME10] M. Mirzargar and A. Entezari. Voronoi splines. *IEEE Transactions on Signal Processing*, 58(9), 2010.
- [OS03] P. Oswald and P. Schröder. Composite primal/dual -subdivision schemes. *Computer Aided Geometric Design*, 20(3):135–164, 2003.
- [PB02] H. Prautzsch and W. Boehm. Box splines. In *Handbook of CAGD*, G. Farin, J. Hoschek, and M.-S. Kim, Eds, page 255282. Elsevier, 2002.
- [PM62] D. P. Petersen and D. Middleton. Sampling and reconstruction of wave-number-limited functions in N -dimensional Euclidean spaces. *Information and Control*, 5(4):279–323, December 1962.
- [vBU⁺04] D. van de Ville, T. Blu, M. Unser, W. Philips, I. Lemahieu, and R. van de Walle. Hex-splines: a novel spline family for hexagonal lattices. *IEEE Trans. Image Proc.*, 13(6):758–772, June 2004.
- [vdVU10] D. van de Ville and M. Unser. Personal communication, Banff, Nov 2010.